ELECTRONIC SUPPLEMENTARY INFORMATION (ESI)

Secondary interactions, steric hindrance and electric charge effect the on the interaction of $V^{IV}O$ species with proteins

Giuseppe Sciortino,[a,b] Daniele Sanna,[c] Valeria Ugone,[b] Jean-Didier Maréchal,[a] Mercè Alemany-Chavarria,[a] and Eugenio Garribba*[b]

[a] *Departament de Química, Universitat Autònoma de Barcelona, 08193 Cerdanyola del Vallés, Barcelona, Spain*

[b] *Dipartimento di Chimica e Farmacia, Università di Sassari, Via Vienna 2, I-07100 Sassari, Italy. E-mail: garribba@uniss.it; Tel: +39 079 229487.*

[c] *Istituto CNR di Chimica Biomolecolare, Trav. La Crucca 3, I-07040 Sassari, Italy.*

Table S1 Species identified in the ESI-MS spectra of the system $V^{IV}O^{2+}$/Hpip 1/2.

Ion	Composition	Exptl m/z [a]	Calcd m/z [a]	Error (ppm) [b]
$[V^{IV}O(pip)_2+H]^+$	$C_{28}H_{33}N_{10}O_7V$	672.19713	672.19678	0.5
$[V^{IV}O(pip)_2(OH)]^-$	$C_{28}H_{33}N_{10}O_8V$	688.19279	688.19352	-1.1
$[V^{V}O_2(pip)_2]^-$	$C_{28}H_{32}N_{10}O_8V$	687.18573	687.18497	1.1

[a] Experimental and calculated m/z values are referred to the peak with monoisotopic mass. [b] Error in ppm respect to the calculated value, obtained as $10^6 \times$ [(m/z experimental – m/z calculated) / m/z calculated].

Table S2 Species identified in the ESI-MS of the of the system $V^{IV}O^{2+}/H_2hqs$ 1/2.

Ion	Composition	Exptl m/z [a]	Calcd m/z [a]	Error (ppm) [b]
$[V^{IV}O(Hhqs)_2+H]^+$	$C_{18}H_{13}N_2O_9S_2V$	515.94982	515.94966	0.3
$[V^{IV}O(Hhqs)_2+Na]^+$	$C_{18}H_{12}N_2O_9S_2VNa$	537.93177	537.93161	0.3
$[V^{IV}O(hqs)_2]^{2-}$	$C_{18}H_{10}N_2O_9S_2V$	256.46395	256.46392	0.1
$[V^{IV}O(Hhqs)(hqs)]^-$	$C_{18}H_{11}N_2O_9S_2V$	513.93554	513.93511	0.8
$[V^{V}O_2(hqs)_2]^{3-}$	$C_{18}H_{10}N_2O_{10}S_2V$	176.30700	176.30776	-4.3

[a] Experimental and calculated m/z values are referred to the peak with monoisotopic mass. [b] Error in ppm respect to the calculated value, obtained as $10^6 \times$ [(m/z experimental – m/z calculated) / m/z calculated].

Table S3 Binding sites for *SPY*-5-13-C-[VO(Hpip)$_2$]$^{2+}$ determined by docking methods.

Ranking [a]	Hbond	Distance [b]	F_{max} [c]	F_{mean} [d]	% Pop.[e]
I	O1⋯Arg72(NH$_2$)	1.950	26.12	25.40	4.0
	O4b⋯Arg42(NH$_2$)	2.116			
	O4b⋯Gln49(NH$_2$)	1.453			
II	O1⋯Arg74(NH$_2$)	1.434	26.04	22.99	6.0
	O4b⋯Arg72(NH$_2$)	2.289			
	N9a⋯Glu24(COO)	1.709			
III	O4a⋯Arg72(NH$_2$)	1.756	23.47	21.98	15.0
	N9b⋯Gly47(CO)	1.534			
IV	O4b⋯Arg72(NH$_2$)	2.145	21.12	18.19	24.0
	N9a⋯Gly47(CO)	1.540			
V	O4b⋯Arg42(NH$_2$)	1.996	21.01	20.40	5.0
	N9a⋯THr7(CO)	2.110			
VI	O4b⋯Arg42(NH$_2$)	1.541	15.82	18.84	10.0
VII	O4a⋯Arg72(NH$_2$)	3.158	14.52	13.05	11.0
	O4b⋯Arg72(NH$_2$)	2.243			
VIII	O4b⋯Arg74(NH$_2$)	2.105	12.41	11.57	7.0
	O4a⋯Lys27(NH$_3$)	4.152			
	O4a⋯Arg72(NH$_2$)	1.928			
	N7b⋯Arg72(NH$_2$)	2.044			

[a] Ranking of the identified cluster. [b] Distance in Å. [c] GoldScore *Fitness* value obtained for the most stable pose of each cluster (F_{max}). [d] Average value of GoldScore *Fitness* for each cluster (F_{mean}). [e] Percentage computed considering the total of the solutions reported (number of solutions per cluster).

Table S4 Binding sites for *SPY*-5-13-A-[VO(Hpip)$_2$]$^{2+}$ determined by docking methods.

Ranking [a]	Hbond	Distance [b]	F_{max} [c]	F_{mean} [d]	% Pop.[e]
I	O4a···Arg74(NH$_2$)	2.521	25.91	24.31	7.0
	O4b···Arg72(NH$_2$)	2.136			
	N9a···Glu24(COO)	1.852			
II	O4a···Arg72(NH$_2$)	1.610	20.86	19.20	26.0
	N9b···Gly47(CO)	1.757			
III	O4a···Arg72(NH$_2$)	1.681	20.77	19.36	21.0
	N9b···Gly47(CO)	1.727			
	N9a···Gly47(CO)	1.583			
IV	O4a···Arg72(NH$_2$)	1.726	20.44	19.78	7.0
	N9b···Gly47(CO)	1.615			
V	O4b···Arg42(NH$_2$)	1.603	12.28	11.42	15.0

[a] Ranking of the identified cluster. [b] Distance in Å. [c] GoldScore *Fitness* value obtained for the most stable pose of each cluster (F_{max}). [d] Average value of GoldScore *Fitness* for each cluster (F_{mean}). [e] Percentage computed considering the total of the solutions reported (number of solutions per cluster).

Table S5 Binding sites for *SPY*-5-12-[VO(Hpip)$_2$]$^{2+}$ determined by docking methods.

Ranking [a]	Hbond	Distance [b]	F_{max} [c]	F_{mean} [d]	% Pop.[e]
I	O4a···Arg42(NH$_2$)	2.287	22.11	21.14	6.0
	N9b···Thr7(CO)	1.746			
II	O1···Asp52(NH)	2.445	21.29	13.66	5.0
	O4a···Arg72(NH$_2$)	2.034			
	O4b···Arg72(NH$_2$)	2.140			
	O4b···Lys27(NH$_3$)	3.377			
III	O1···Arg42(NH$_2$)	2.219	21.24	19.74	15.0
	N9a···Leu73(CO)	1.452			
	N9b···Thr7(CO)	1.951			
IV	O1···Arg72(NH$_2$)	1.506	21.08	20.28	4.0
	O4a···Arg42(NH$_2$)	3.656			
	O4a···Gln49(NH$_2$)	1.807			
	N9a···Glu24(COO)	2.314			
V	N9a···Thr7(CO)	1.654	19.36	18.61	24.0
	N9b···Leu73(CO)	1.686			
VI	N9a···Leu73(CO)	1.955	19.07	18.70	10.0
	N9b···Thr7(CO)	1.506			
VII	O4a···Lys6(NH$_3$)	3.291	18.82	18.13	4.0
VIII	N7b···Arg72(NH$_2$)	2.135	18.80	17.81	7.0
	N9a···Glu24(COO)	1.837			

[a] Ranking of the identified cluster. [b] Distance in Å. [c] GoldScore *Fitness* value obtained for the most stable pose of each cluster (F_{max}). [d] Average value of GoldScore *Fitness* for each cluster (F_{mean}). [e] Percentage computed considering the total of the solutions reported (number of solutions per cluster).

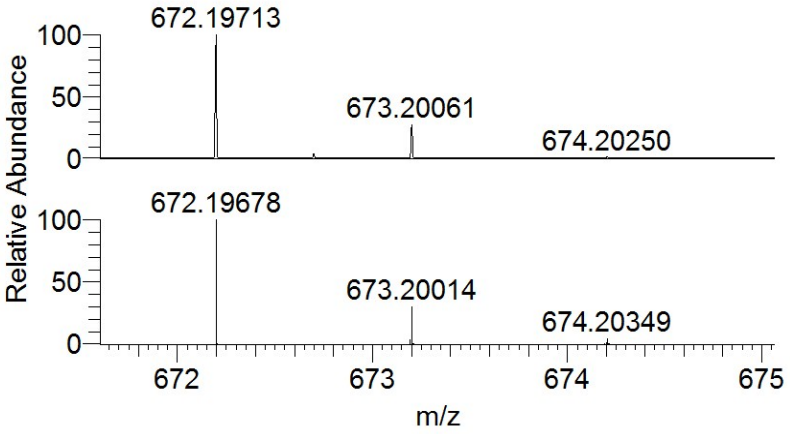

Fig. S1 Experimental (top) and calculated (bottom) isotopic pattern for the peak of $[V^{IV}O(pip)_2+H]^+$ revealed at m/z = 672.20 in the ESI-MS spectrum of the system $V^{IV}O^{2+}$/Hpip 1/2 recorded in the positive-ion mode with a V concentration of 50 μM.

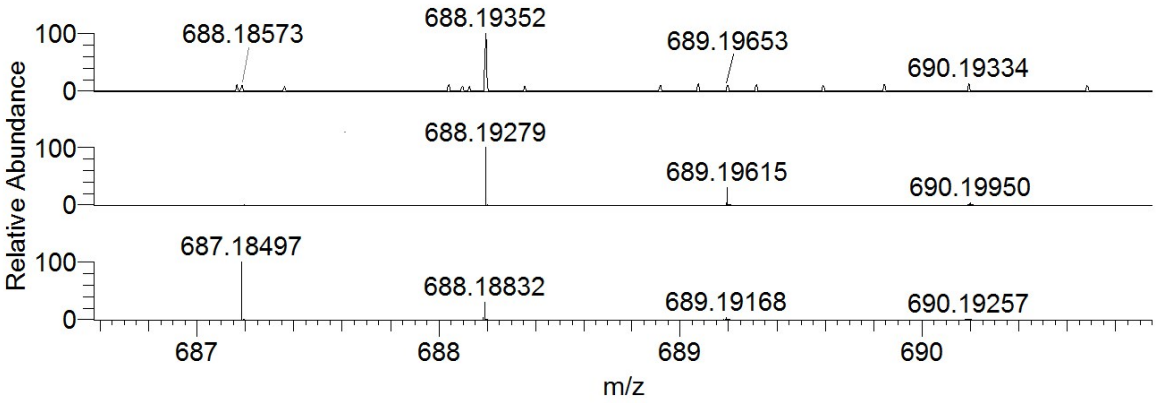

Fig. S2 Experimental (top) and calculated isotopic pattern for the peak of $[V^{IV}O(pip)_2(OH)]^-$ (center) and of $[V^{V}O_2(pip)_2]^-$ (bottom) revealed respectively at m/z = 688.19 and 687.18 in the ESI-MS spectrum of the system $V^{IV}O^{2+}$/Hpip 1/2 recorded in the negative-ion mode with a V concentration of 50 μM.

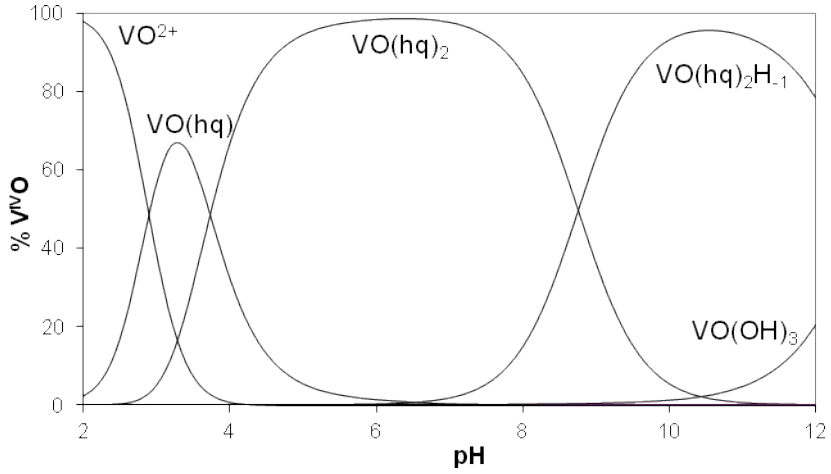

Fig. S3 Distribution diagram of the complexes formed in the system containing $V^{IV}O^{2+}$ and 8-hydroxyquinoline (Hhq) as a function of pH at molar ratio 1:2 ($V^{IV}O^{2+}$ 1 mM). Figure adapted from E. Garribba, G. Micera, D. Sanna and E. Lodyga-Chruscinska, *Inorg. Chim. Acta*, 2003, **348**, 97-106.

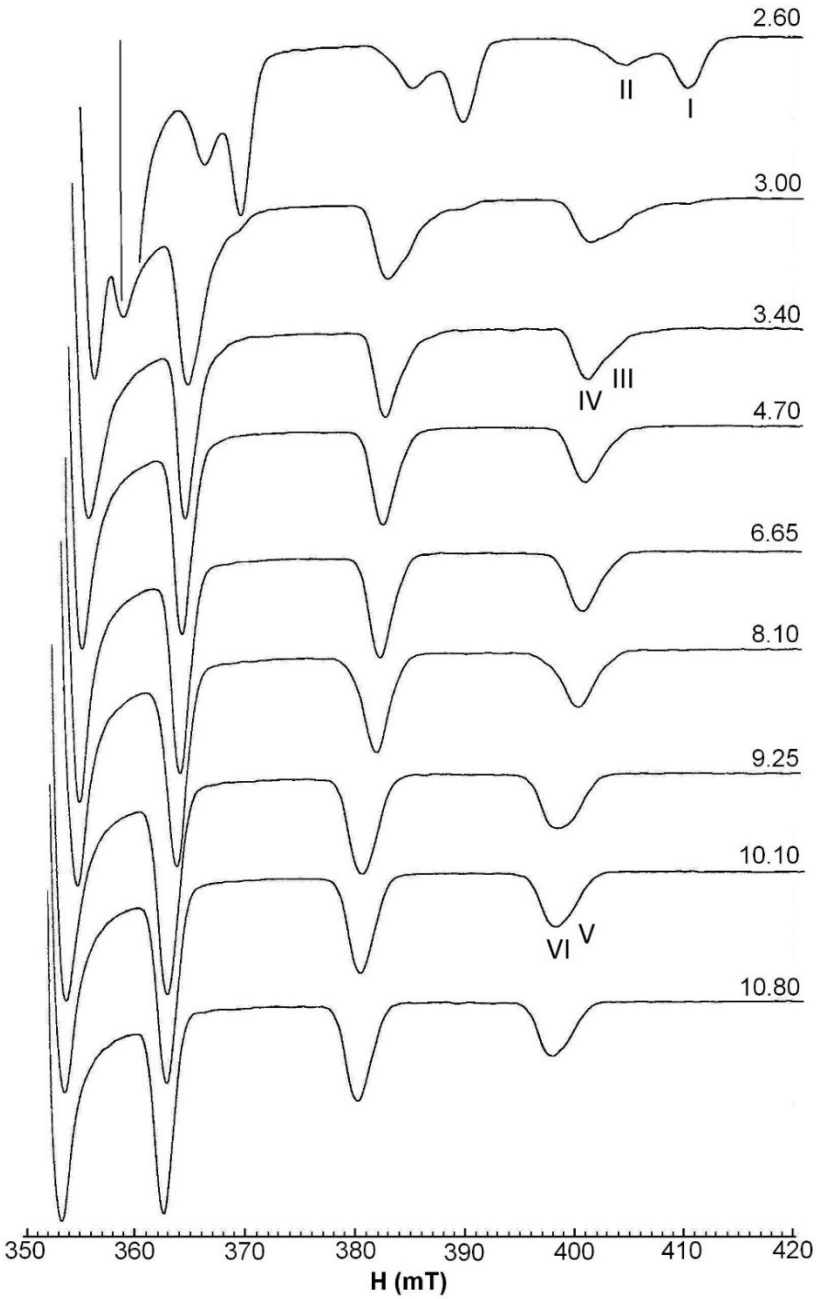

Fig. S4 High field region of the anisotropic EPR spectra recorded on frozen aqueous solutions (120 K) with varying pH of the system $V^{IV}O^{2+}/H_2hqs$ at molar ratio 1/2 ($V^{IV}O^{2+}$ 4 mM). Figure adapted from E. Garribba, G. Micera, D. Sanna and E. Lodyga-Chruscinska, *Inorg. Chim. Acta*, 2003, **348**, 97-106.

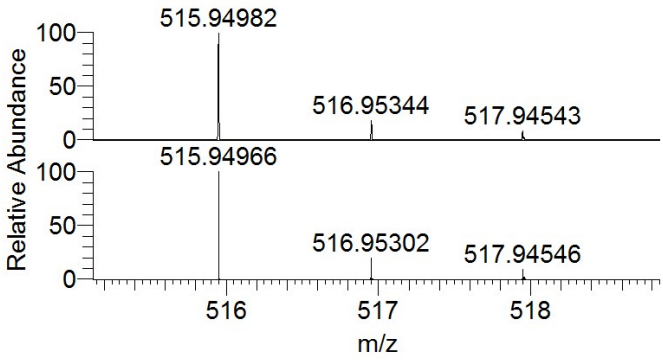

Fig. S5 Experimental (top) and calculated (bottom) isotopic pattern for the peak of $[VO(Hhqs)_2+H]^+$ revealed at m/z = 515.95 in the ESI-MS spectrum of the system $V^{IV}O^{2+}/H_2hqs$ 1/2 recorded in the positive-ion mode with a V concentration of 50 μM.

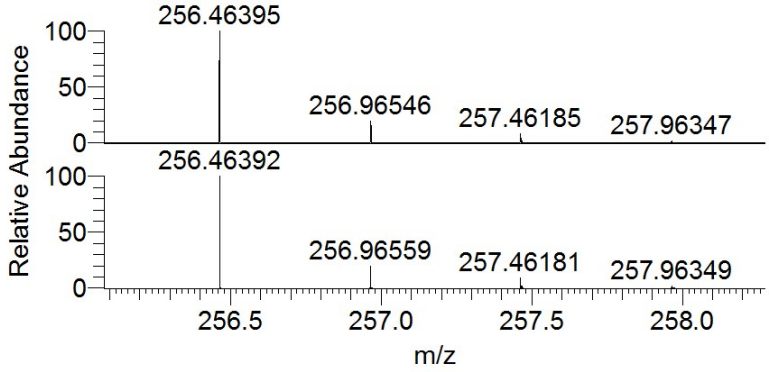

Fig. S6 Experimental (top) and calculated (bottom) isotopic pattern for the peak of $[V^{IV}O(hqs)_2]^{2-}$ revealed at m/z = 256.46 in the ESI-MS spectrum of the system $V^{IV}O^{2+}/H_2hqs$ 1/2 recorded in the negative-ion mode with a V concentration of 50 μM.

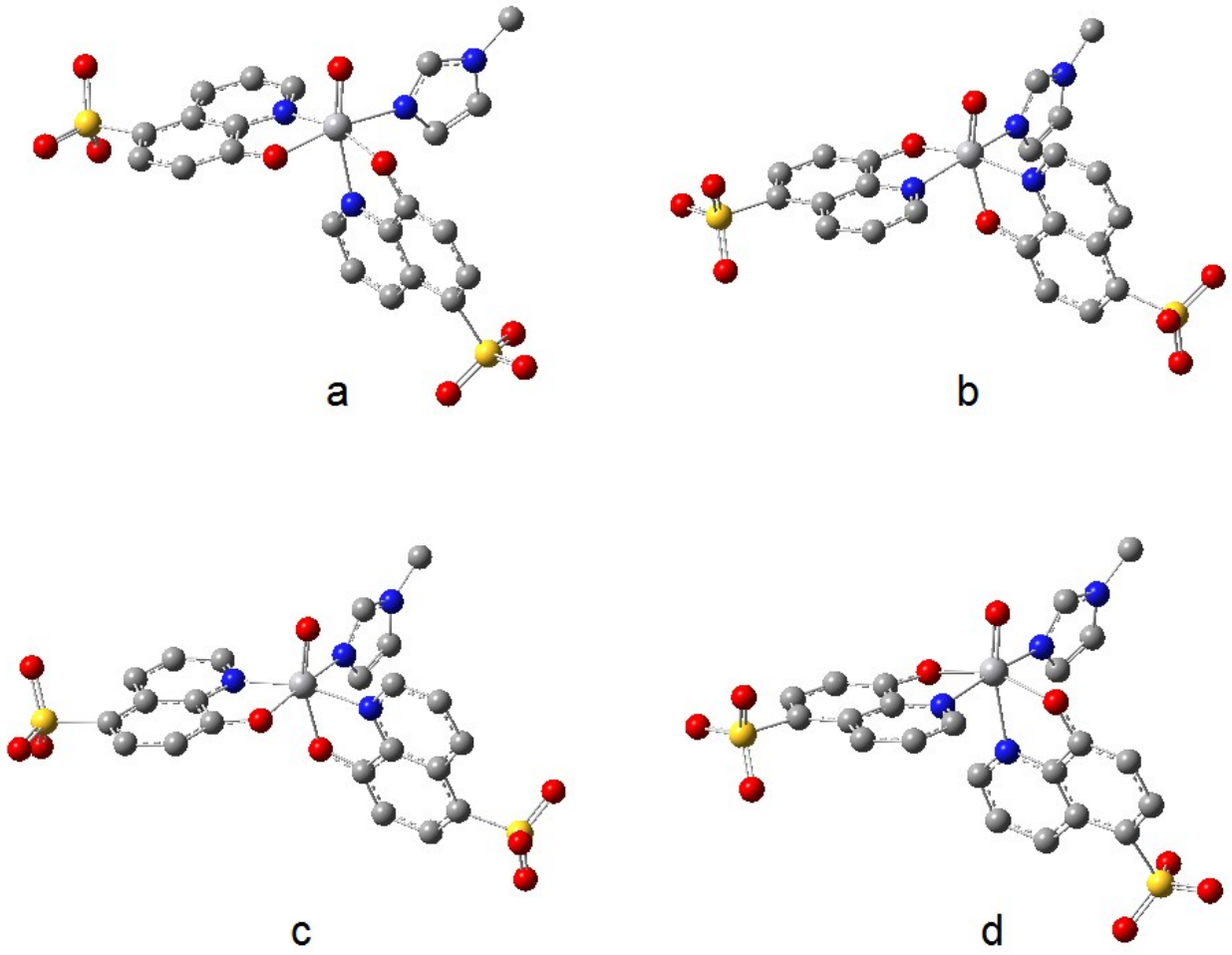

Fig. S7 Optimized structures of the possible isomers of *cis*-$[VO(hqs)_2(MeIm)]^{2-}$ formed by $V^{IV}O^{2+}$, H_2hqs and MeIm: a) *OC*-6-44; b) *OC*-6-24; c) *OC*-6-23; d) *OC*-6-42. Hydrogen atoms are omitted for clarity.

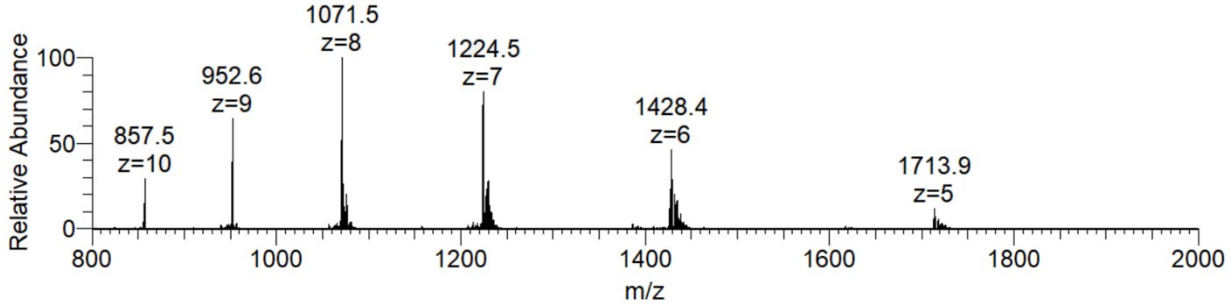

Fig. S8 ESI-MS spectrum of ubiquitin (50 μM).

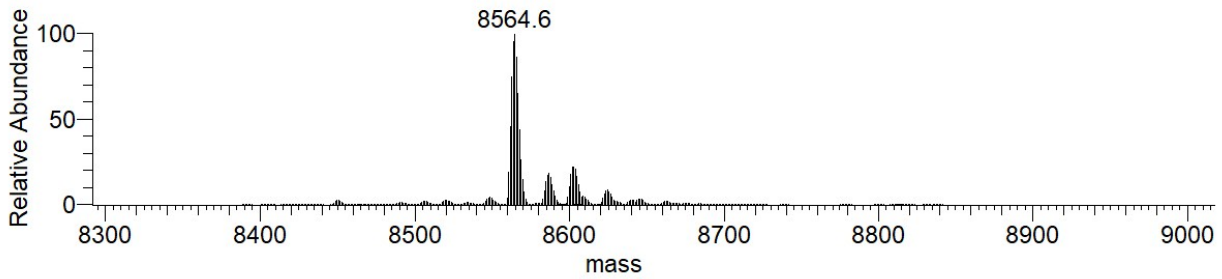

Fig. S9 Deconvoluted ESI-MS spectrum of ubiquitin (50 μM).

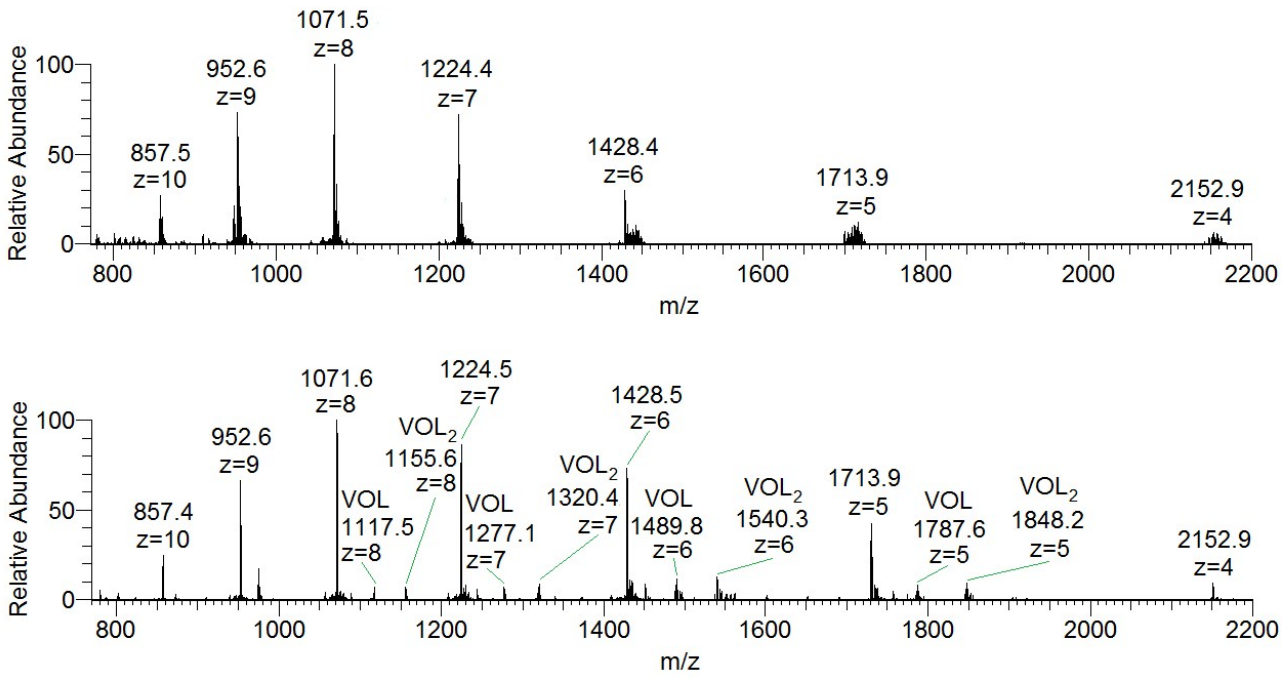

Fig. S10 Full ESI-MS spectra recorded in the systems with Ub (top) and with $V^{IV}O^{2+}$/Hpip/Ub (bottom). Ub concentration was 50 μM and molar ratio V/Ub was 3/1. The peaks due to the formation of the adducts between VOL and VOL_2 moieties and Ub are also shown.

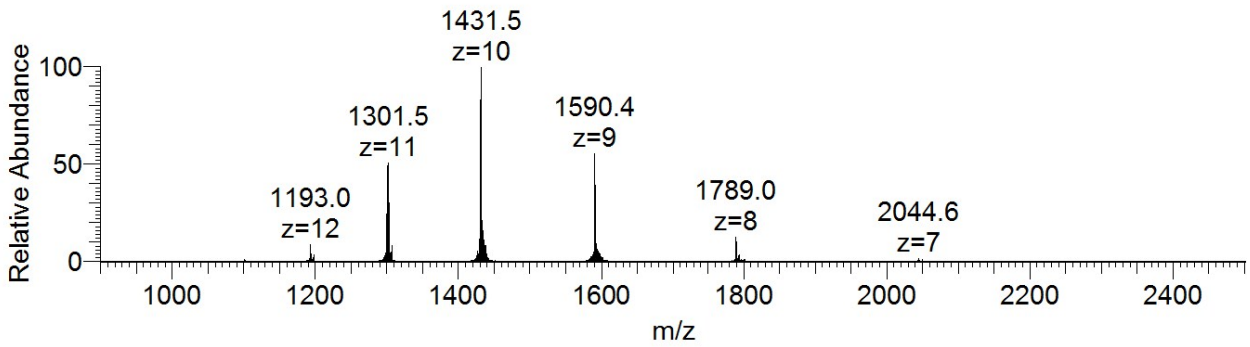

Fig. S11 ESI-MS spectrum of lysozyme (50 μM).

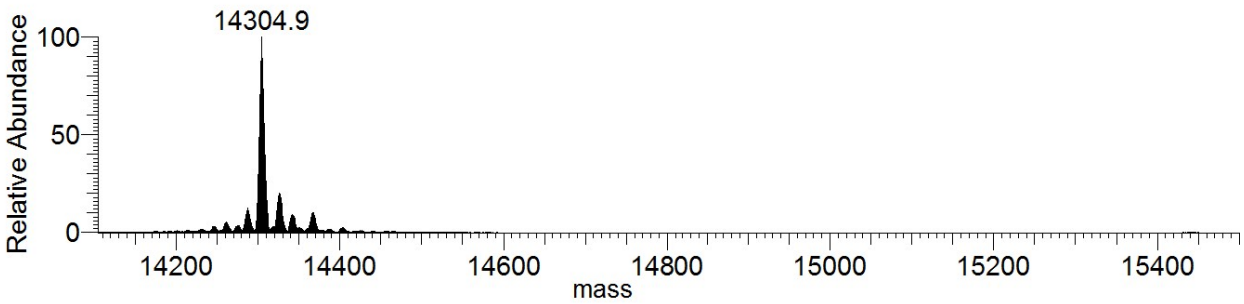

Fig. S12 Deconvoluted ESI-MS spectrum of lysozyme (50 μM).

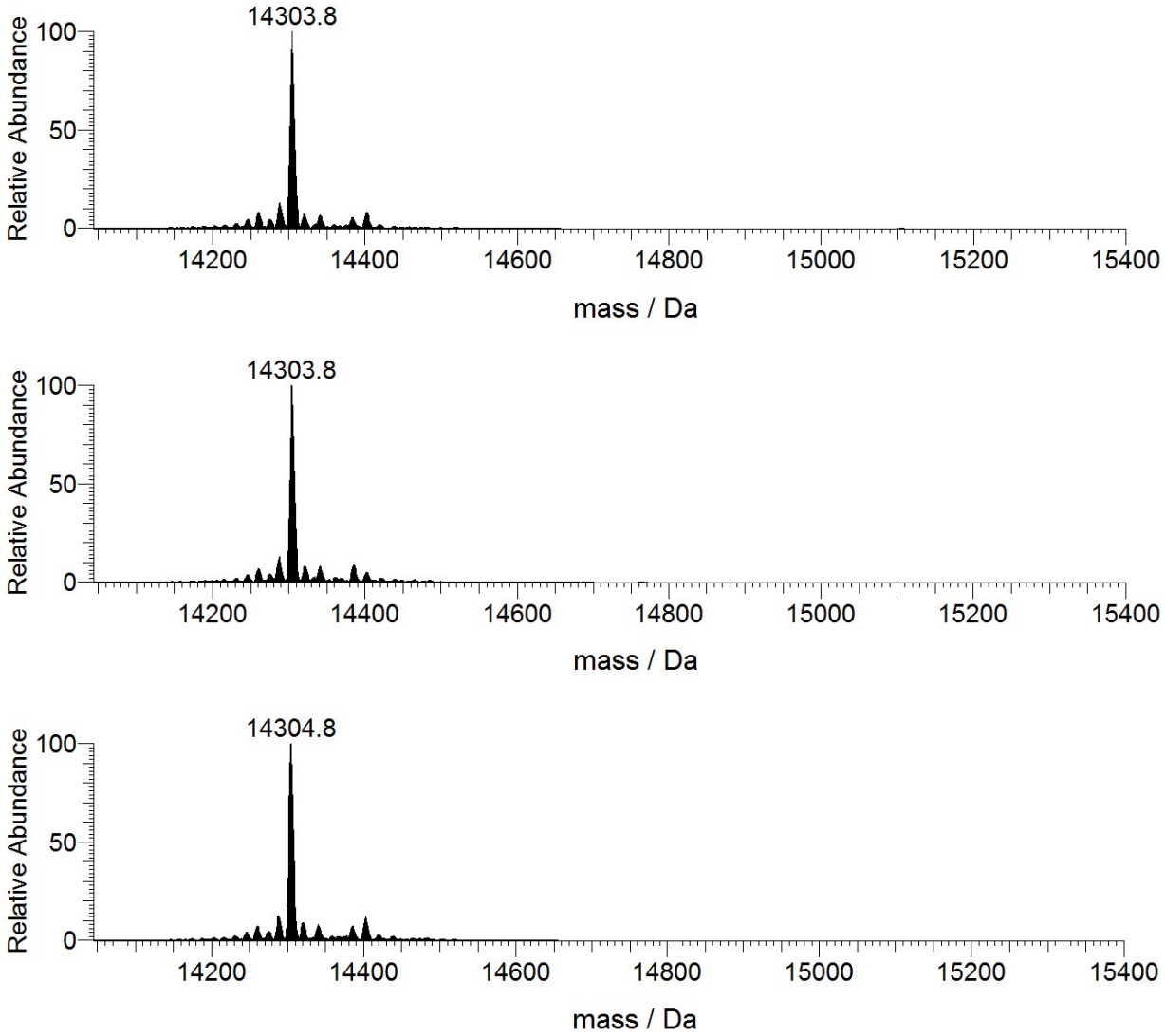

Fig. S13 Deconvoluted ESI-MS spectra recorded on the system containing $V^{IV}O^{2+}$/Hpip 1/2 and lysozyme (50 μM): molar ratio V/Lyz 2/1 (top), 3/1 (center) and 5/1 (bottom).

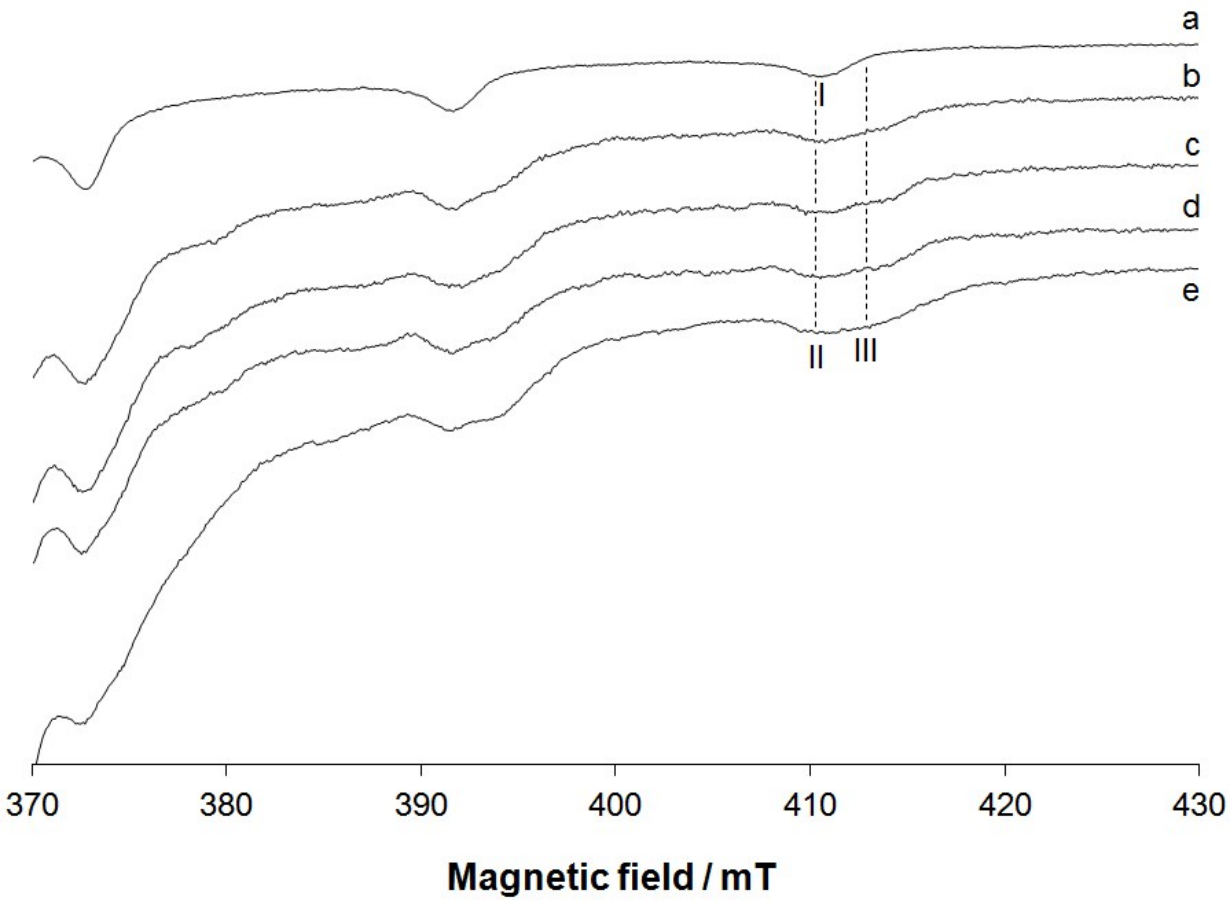

Fig. S14 High field region of the anisotropic EPR spectra recorded on frozen solutions (120 K) containing: a) $V^{IV}O^{2+}$/Hpip/MeIm 1/2/4; b) $V^{IV}O^{2+}$/Hpip/Lyz 1/2/1; c) $V^{IV}O^{2+}$/Hpip/Lyz 2/4/1; d) $V^{IV}O^{2+}$/Hpip/Lyz 3/6/1; e) $V^{IV}O^{2+}$/Hpip 1/2. $V^{IV}O^{2+}$ concentration was 1.0×10^{-3} M in all the systems. The M_I = 7/2 resonances of $[VO(Hpip)_2(MeIm)]^{2+}$, $[VO(Hpip)_2]^{2+}$ and *cis*-$[VO(Hpip)_2(H_2O)]^{2+}$ are indicated with **I**, **II** and **III**. The resonances of the binary species $[VO(Hpip)_2]^{2+}$ and *cis*-$[VO(Hpip)_2(H_2O)]^{2+}$ are also denoted with the dotted lines.

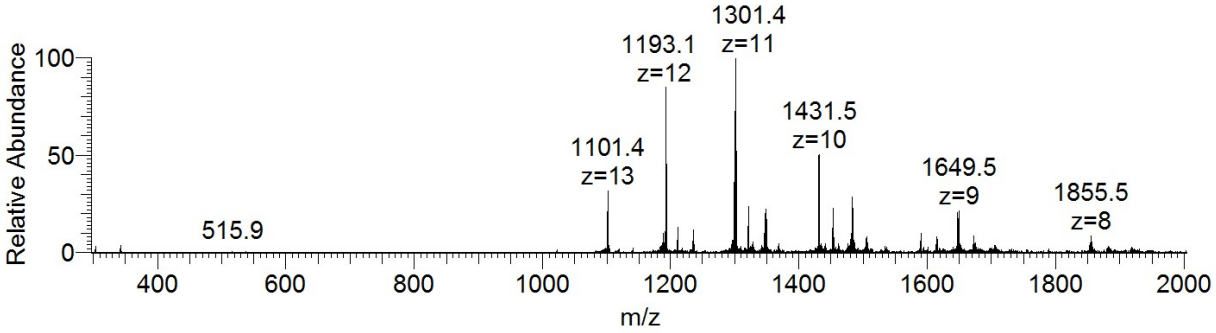

Fig. S15 ESI-MS spectrum recorded on the system containing $V^{IV}O^{2+}/H_2hqs$ 1/2 and lysozyme (50 μM) with molar ratio V/Lyz 4/1.